

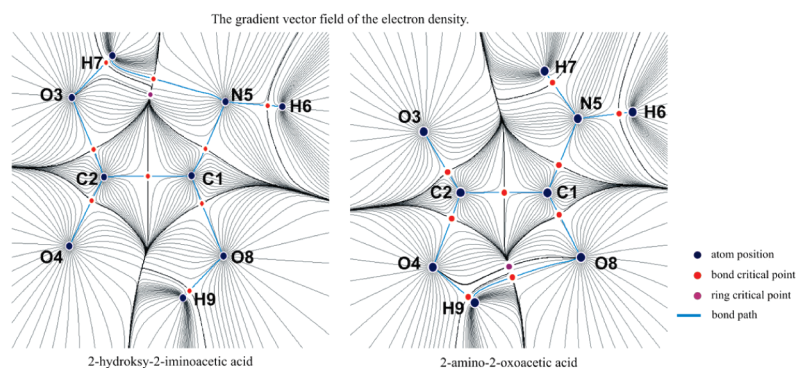
Intramolecular Double Proton Transfer from 2-Hydroxy-2-iminoacetic Acid to 2-Amino-2-oxoacetic Acid

Barbara Bankiewicz,[†] Sławomir Wojtulewski,^{*†} and Sławomir J. Grabowski^{*‡}

[†]*Institute of Chemistry, University of Białystok, ul. Hurtowa 1, 15-399 Białystok, Poland, and*
[‡]*Ikerbasque Research Professor, Kimika Fakultatea, Euskal Herriko Unibertsitatea and Donostia International Physics Center (DIPC), P.K. 1072, 20080 Donostia, Euskadi, Spain*

s.wojtulewski@uwb.edu.pl; s.grabowski@ikerbasque.org

Received October 23, 2009



The double intramolecular proton transfer process which transforms 2-hydroxy-2-iminoacetic acid into 2-amino-2-oxoacetic acid is analyzed. The MP2 and DFT calculations were performed for different tautomers and conformers of these species. Pople style (6-311++G(d,p), 6-311++G-3(d,f,3p,d)) and Dunning type (aug-cc-pVTZ) basis sets were applied. O–H···O, N–H···O, and O–H···N intramolecular hydrogen bonds were also analyzed with the use of Quantum Theory of “Atoms in Molecules” (QTAIM) as well as Natural Bond Orbitals (NBO) method. Different criteria of the hydrogen bonding existence were applied here for intramolecular interactions. It was found that some of N–H···O hydrogen bonds may be treated as blue-shifting ones.

Introduction

Proton transfer (PT) reaction plays a meaningful role in numerous and complex physical, chemical, and biochemical processes.¹ It was analyzed in detail for many complexes connected through intermolecular hydrogen bonds. For example, the double proton transfer was investigated both theoretically and experimentally for the centrosymmetric dimer of formic acid.² Other carboxylic acids connected through two equivalent hydrogen bonds were also investigated.³ If the products of proton transfer are the same and are geometrically equivalent to the reactants, then a

symmetrical double potential energy well corresponding to this process exists.⁴ There are numerous examples such as the aforementioned formic acid dimer, complexes of the hydronium ion with the water molecule ($\text{H}_2\text{OH}^+ + \text{OH}_2 \rightleftharpoons \text{H}_2\text{O} + {}^+\text{HOH}_2$), and many other cases.⁵ Frequently for heteronuclear hydrogen bonds, the proton transfer leads to different tautomeric forms or even to different species, e.g., $\text{CH}_3\text{CN} + \text{H}_3\text{O}^+ \rightleftharpoons \text{CH}_3\text{CNH}^+ + \text{H}_2\text{O}$.⁶ The centrosymmetric dimers of formamide and related species where two equivalent N–H···O hydrogen bonds occur are the other examples of the existence of a nonsymmetric potential energy well.⁷ For the latter complexes, the products of the double PT

(1) (a) Cleland, W. W.; Kreevoy, M. M. *Science* **1994**, *264*, 1887. (b) Perrin, C. L.; Nielson, J. B. *Annu. Rev. Phys. Chem.* **1997**, *48*, 511.
(2) Kim, Y. *J. Am. Chem. Soc.* **1996**, *118*, 1522.
(3) Loerting, T.; Liedl, K. R. *J. Am. Chem. Soc.* **1998**, *120*, 12595.
(4) *Hydrogen-Transfer Reactions*; Hynes, J. T., Klinman, J. P., Limbach, H.-H., Schowen, R. L., Eds.; Wiley-VCH Verlag GmbH & Co. KGaA: Weinheim 2007.

(5) (a) Huang, X.; Cho, H. M.; Carter, S.; Ojamäe, L.; Bowman, J. M.; Singer, S. J. *J. Phys. Chem. A* **2003**, *107*, 7142. (b) Stoyanov, E. S.; Reed, C. A. *J. Phys. Chem. A* **2006**, *110*, 12992.

(6) Gardénier, G. H.; Roscioli, J. R.; Johnson, M. A. *J. Phys. Chem. A* **2008**, *112*, 12022.

(7) Grabowski, S. J.; Sokalski, W. A.; Leszczynski, J. *J. Phys. Chem. A* **2006**, *110*, 4772.

process containing O–H···N hydrogen bonds are the tautomeric forms of the reactants.

There are numerous factors that characterize the hydrogen bonding interaction. One of them concerns the geometry of H-bridges. It is well-known that the X–H···Y system (X is the proton donor while Y is the proton acceptor) tends to be linear since such geometrical arrangement is in line with the most effective electron charge transfer from the acceptor to the proton donating bond.⁸ In other words, such an arrangement favors the $n \rightarrow \sigma^*$ electron charge transfer with the corresponding energy within the Natural Bond Orbitals (NBO) approach,⁹ where n designates the lone electron pair of an acceptor center while σ^* is a proton donating bond's antibonding orbital. The energy of such a transfer may be also treated as an indicator of the hydrogen bonding strength.

It was stated that the strongest hydrogen bonds are linear or nearly so. Such geometrical requirements may not be fulfilled for intramolecular hydrogen bonds where the proton–proton acceptor (H···Y) short distances suffer from energy constraints.¹⁰ Hence, for intramolecular interactions the existence of the hydrogen bonding is often ambiguous. For example, recent studies on intramolecular dihydrogen bonds show that for some species the Quantum Theory of “Atoms in Molecules”¹¹ does not indicate the existence of the hydrogen bonding while NBO analysis⁹ clearly shows that the hydrogen bond occurs.¹²

The proton transfer reaction for intramolecular hydrogen bonds is another interesting effect often characterized by quite different mechanisms than those known for intermolecular processes. The intramolecular PT was investigated in numerous studies on pseudo six-membered rings,¹³ especially for those interactions which may be classified as Resonance Assisted Hydrogen Bonds (RAHBs).¹⁴ For the latter systems, the single- and double-conjugated covalent bonds exist with an additional H···Y connection, e.g., malonaldehyde and its derivatives. The RAHBs of O–H···O and N–H···O bonds were investigated theoretically and experimentally, and numerous crystal structures containing RAHBs have also been detected. There are also studies on the different types of RAHBs, e.g., O–H···S, S–H···S, and N–H···S.¹⁵ The idea of RAHB systems has been criticized recently.¹⁶ However, it should be mentioned that the π -electron delocalization for the cited above systems

with conjugated single and double bonds leads to the enhancement of the hydrogen bonding strength.¹⁷ Sometimes such interactions are very strong with the proton movement close to the middle of the X···Y distance. Such an effect was mainly observed for O–H···O bonds.¹⁸ Very strong hydrogen bonds are classified as Low Barrier Hydrogen Bonds (LBHBs) or Short-Strong Hydrogen Bonds (SSHBs).¹⁹ For those species, the proton transfer barrier height is very low or a single potential well exists with the proton position in the center of the H-bridge. Numerous studies were performed for six-membered rings connected through the intramolecular hydrogen bonding. Different proton donors and different proton acceptors were considered for the latter hydrogen bonds and various methods and techniques were applied, among them QTAIM¹¹ and NBO.⁹

Another topic investigated concerns the interrelation between H-bond interaction and the proton transfer reaction. It has been pointed out that the hydrogen bonding is the first and preliminary step of the proton transfer process.²⁰ However, this theory has been contested since there is no direct relation between both phenomena.²¹ In other words, neither the existence of the hydrogen bonding implies the PT reaction nor the strength of such interaction correlates with any characteristic of this process. On the other hand, it was found that various chemical reactions and processes may be analyzed by the crystal structures' results since it was stated that a proper fragment of the crystal structure may be treated as a frozen stage of any chemical reaction.²² Hence, for example, the $-\text{C}=\text{O}\cdots\text{H}-\text{O}-\text{C}- \rightleftharpoons -\text{C}-\text{O}-\text{H}\cdots\text{O}=\text{C}-$ process may be analyzed in this way since the crystal neutron diffraction structures contain different $-\text{C}=\text{O}\cdots\text{H}-\text{O}-\text{C}-$ geometrical fragments corresponding to different stages of this proton transfer reaction.¹⁷ It was found that the crystal experimental data are in line with high level ab initio calculations performed on the formic acid dimer and the double proton transfer for the latter system.¹⁷

The question arises if the double intramolecular PT process exists. That matter was partially investigated for 2,4-dihydroxybut-2-ene-4-dial molecule and its simple derivatives²³ conformations containing two connected six-membered rings with two intramolecular hydrogen bonds occasionally arise. It is well-known that the intramolecular hydrogen bonds for six-membered rings are very stable and they occur very often, for example in the crystal structures of organic compounds.²⁴ Hence, the existence of two hydrogen bonds for 2,4-dihydroxybut-2-ene-4-dial is not unexpected. The other challenging problem is the double proton transfer for species containing two pseudo five-membered rings created owing to the existence of intramolecular hydrogen bonds since such systems are expected to be less stable than in

(8) Pimentel, G.; McClellan, A. *The hydrogen bond*; Freeman: San Francisco, 1960.

(9) Weinhold, F.; Landis, C. *Valency and Bonding, A Natural Bond Orbital Donor – Acceptor Perspective*; Cambridge University Press: Cambridge, 2005.

(10) Buemi, G. Intramolecular Hydrogen Bonds. Methodologies and Strategies for Their Strength Evaluation. In *Hydrogen Bonding – New Insights*; Grabowski, S. J., Ed.; Vol.3 of the series: Challenges and Advances in Computational Chemistry and Physics, Leszczynski, J., Ed.; Springer: New York, 2006.

(11) Bader, R. F. W. *Atoms in Molecules. A Quantum Theory*; Oxford University Press: New York, 1990.

(12) Alkorta, I.; Elguero, J.; Grabowski, S. J. *J. Phys. Chem. A* **2008**, *112*, 2721.

(13) Cuma, M.; Scheiner, S.; Kar, T. *THEOCHEM* **1999**, *467*, 37.

(14) Gilli, P.; Bertolasi, V.; Ferretti, V.; Gilli, G. *J. Am. Chem. Soc.* **1994**, *116*, 909.

(15) (a) González, L.; Mó, O.; Yáñez, M. *J. Org. Chem.* **1999**, *64*, 2314.

(b) Wojtulewski, S.; Grabowski, S. J. *Chem. Phys. Lett.* **2003**, *378*, 388.

(c) Sanz, P.; Yáñez, M.; Mó, O. *J. Phys. Chem. A* **2002**, *106*, 4661.

(16) (a) Alkorta, I.; Elguero, J.; Mó, O.; Yáñez, M.; Del Bene, J. E. *Mol. Phys.* **2004**, *102*, 2563. (b) Alkorta, I.; Elguero, J.; Mó, O.; Yáñez, M.; Del Bene, J. E. *Chem. Phys. Lett.* **2002**, *411*, 411.

(17) Sobczyk, L.; Grabowski, S. J.; Krygowski, T. M. *Chem. Rev.* **2005**, *105*, 3513.

(18) (a) Madsen, G. K. H.; Iversen, B. B.; Larsen, F. K.; Kapon, M.; Reisner, G. M.; Herstein, F. H. *J. Am. Chem. Soc.* **1998**, *120*, 10040. (b) Schiött, B.; Iversen, B. B.; Madsen, G. K. H.; Bruice, T. C. *J. Am. Chem. Soc.* **1998**, *120*, 12117.

(19) Remer, R. C.; Jensen, J. H. *J. Phys. Chem. A* **2000**, *104*, 9266.

(20) Bürgi, H.-B.; Dunitz, J. D. *Acc. Chem. Res.* **1983**, *16*, 153.

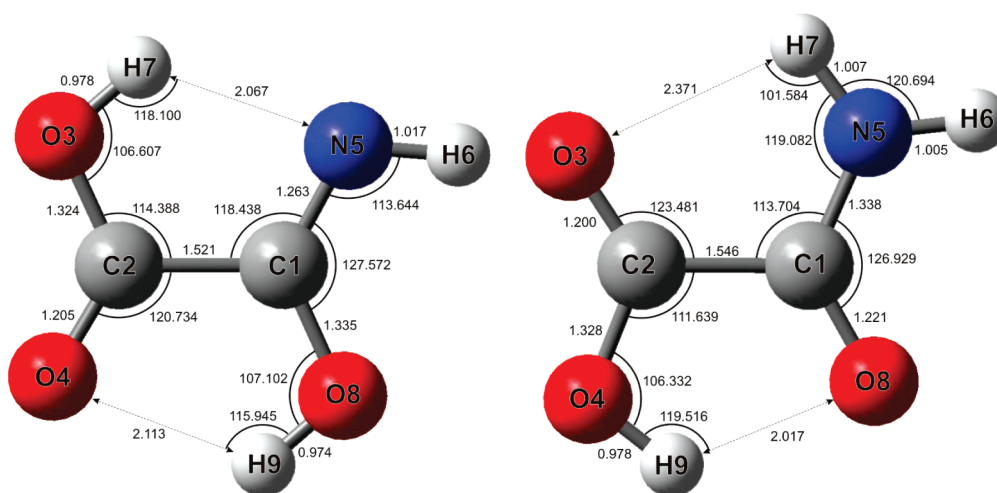
(21) Alkorta, I.; Rozas, I.; Mó, O.; Yáñez, M.; Elguero, J. *J. Phys. Chem. A* **2001**, *105*, 7481.

(22) (a) Dunitz, J. D. *X-Ray Analysis and the Structure of Organic Molecules*; Cornell University Press: Ithaca, 1979. (b) Bürgi, H.-B. *Angew. Chem., Int. Ed.* **1975**, *14*, 460.

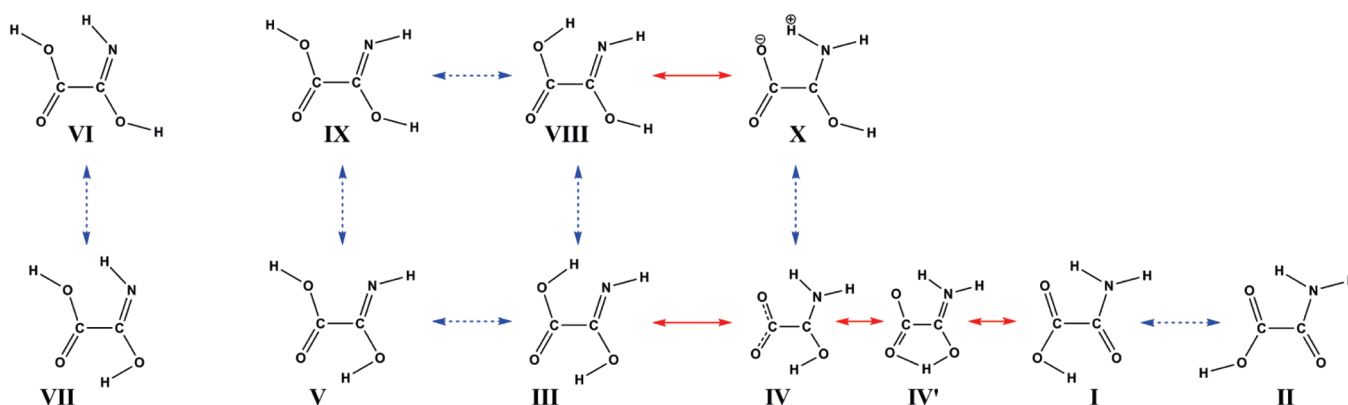
(23) Wojtulewski, S. W.; Grabowski, S. J. *THEOCHEM* **2003**, *621*, 285.

(24) Etter, M. C. *Acc. Chem. Res.* **1990**, *23*, 120.

SCHEME 1



SCHEME 2



the case of six-membered rings. This problem of the double PT was analyzed for the monothiooxalic acid. In this case, two five-membered rings were closed by two $\text{O}-\text{H}\cdots\text{O}$ and $\text{S}-\text{H}\cdots\text{O}$ (or $\text{O}-\text{H}\cdots\text{O}$ and $\text{O}-\text{H}\cdots\text{S}$) hydrogen bonds.²⁵ The reaction paths corresponding to the latter reaction were considered and the possibility of the process occurring in one stage or several stages was discussed. The intramolecular double proton transfer in the excited state of (2,2'-bipyridyl)-3,3'-diol was very recently analyzed experimentally.²⁶

The goal of this study is to analyze the possible conformers of 2-hydroxy-2-iminoacetic acid and 2-amino-2-oxoacetic acid. The discussion on the double proton transfer processes for the latter species is also performed. It simply represents the interchange from 2-hydroxy-2-iminoacetic acid into 2-amino-2-oxoacetic acid. Ab initio and DFT calculations were performed and NBO⁹ and QTAIM¹¹ analyses carried out to characterize the aforementioned conformers and the intramolecular interactions.

Computational Details

The calculations have been carried out with the Gaussian03 set of codes.²⁷ The 2-hydroxy-2-iminoacetic acid and its tautomeric form 2-amino-2-oxoacetic acid were optimized using DFT and ab initio methods. Scheme 1 presents both tautomeric forms with the bond lengths and angles included (B3LYP/aug-cc-pVTZ results). The calculations were carried out at the following levels of approximation: MP2/6-311++G(d,p), B3LYP/6-311++G(d,p), B3LYP/6-311++G(3df,3pd) and B3LYP/aug-cc-pVTZ. Intrinsic reaction coordinate (IRC) paths,²⁸ which connect pairs of conformers or tautomers with the corresponding transition states, were carried out here. Scheme 2 presents the species considered in this study with the indication of all the processes which transform one conformer

(25) Raynaud, C.; Daudey, J.-P.; Maron, L.; Jolibois, F. *J. Phys. Chem. A* **2005**, *109*, 9646.

(26) Stock, K.; Schriever, C.; Lochbrunner, S.; Riedle, E. *Chem. Phys.* **2008**, *349*, 197.

(27) Frisch, M. J.; Trucks, G. W.; Schlegel, H. B.; Scuseria, G. E.; Robb, M. A.; Cheeseman, J. R.; Montgomery, J. A., Jr.; Vrevenban, T.; Kudin, K. N.; Burant, J. C.; Millam, J. M.; Iyengar, S. S.; Tomasi, J.; Barone, V.; Mennucci, B.; Cossi, M.; Scalmani, G.; Rega, N.; Petersson, G. A.; Nakatsuji, H.; Hada, M.; Ehara, M.; Toyota, K.; Fukuda, R.; Hasegawa, J.; Ishida, M.; Nakajima, T.; Honda, Y.; Kitao, O.; Nakai, H.; Klene, M.; Li, X.; Knox, J. E.; Hratchian, H. P.; Cross, J. B.; Adamo, C.; Jaramillo, J.; Gomperts, R.; Stratmann, R. E.; Yazyev, O.; Austin, A. J.; Cammi, R.; Pomelli, C.; Ochterski, J. W.; Ayala, P. Y.; Morokuma, K.; Voth, G. A.; Salvador, P.; Dannenberg, J. J.; Zakrzewski, V. G.; Dapprich, S.; Daniels, A. D.; Strain, M. C.; Farkas, O.; Malick, D. K.; Rabuck, A. D.; Raghavachari, K.; Foresman, J. B.; Ortiz, J. V.; Cui, Q.; Baboul, A. G.; Clifford, S.; Cioslowski, J.; Stefanov, B. B.; Liu, G.; Liashenko, A.; Piskorz, P.; Komaromi, I.; Martin, R. L.; Fox, D. J.; Keith, T.; Al-Laham, M. A.; Peng, C. Y.; Nanayakkara, A.; Challacombe, M.; Gill, P. M. W.; Johnson, B.; Chen, W.; Wong, M. W.; Gonzalez, C.; Pople, J. A. *Gaussian 03, Revision B.03*, Gaussian, Inc., Pittsburgh PA, 2003.

(28) (a) Gonzalez, C.; Schlegel, H. B. *J. Chem. Phys.* **1989**, *90*, 2154.
(b) Gonzalez, C.; Schlegel, H. B. *J. Phys. Chem.* **1990**, *94*, 5523.

(or tautomer) into the other one. Continuous lines show the proton transfer processes while the dashed ones designate rotations. All species presented here correspond to stationary points, except of IV and IV' being only the special structures found on IRC paths. Those paths correspond to transition states of III \rightarrow I and X \rightarrow I reactions. It is worth mentioning that only at the B3LYP/6-311++G(d,p) level of approximation the conformation IV is a local minimum while IV' is TS of the IV \rightarrow I process; for the remaining levels of approximation TS III-I is the transition state of the III \rightarrow I proton transfer.

The NBO method^{9,29} implemented within the Gaussian03 package was also applied to calculate the atomic charges and $n_Y \rightarrow \sigma_{XH}^*$ interaction energies. This interaction is responsible for the existence of the X-H...Y hydrogen bonding. n_Y designates the lone electron pair of the Y proton acceptor and σ_{XH}^* is an antibonding orbital of the X-H proton donating bond. The $n_Y \rightarrow \sigma_{XH}^*$ interaction is calculated as second order perturbation theory energy according to the following equation:

$$\Delta E(n_Y \rightarrow \sigma_{XH}^*) = -2\langle n_Y | F | \sigma_{XH}^* \rangle^2 / (\epsilon(\sigma_{XH}^*) - \epsilon(n_Y)) \quad (1)$$

$\langle n_Y | F | \sigma_{XH}^* \rangle$ is the Fock matrix element and $(\epsilon(\sigma_{XH}^*) - \epsilon(n_Y))$ is the orbital energy difference.

The QTAIM theory of Bader was also applied to locate critical points^{11,30} and to analyze them in terms of electron densities and their Laplacians.

Results and Discussion

Energetic and Geometrical Parameters. There are numerous studies on different kinds of proton transfer reactions.⁴ The multiproton transfer has often been investigated. It was previously mentioned here that the double proton transfer reaction for carboxylic acid dimers is a very well-known process and has been described from experimental and theoretical points of view.^{2,3} However, the intramolecular double proton transfer can also occur. This mechanism was considered in the case of intramolecular double PT for porphine, porphycene, or naphthazarin.³¹ The studies on the PT reaction for simple systems containing at most several atoms are very interesting. They may explain mechanisms of such processes for large biochemical systems.

For simple systems, a deeper insight into various energetic, geometrical and QTAIM parameters is possible. However, the number of studies on intramolecular double PT for very simple species is rather restricted. One may mention the recent study on monothiooxalic acid, for which two types of the proton transfer may be indicated (1,3- and 1,4-prototropy).²⁵ For the latter reactions there are five-membered rings connected through intramolecular hydrogen bonds. In spite of the simplicity of these systems the PT processes are equivocal.

Species analyzed here: 2-hydroxy-2-iminoacetic acid (III, Scheme 2) and 2-amino-2-oxoacetic acid (I, Scheme 2) were similar to aforementioned. The two intramolecular hydrogen bonds occur in both molecules. To analyze reaction paths for the intramolecular double PT which interchanges III into I, the calculations for different conformations and

TABLE 1. Energies (in kcal/mol) of Analyzed Conformations Related to the Conformation I (the Lowest Energy) (DFT and MP2 Results with the Use of Different Basis Sets Are Presented)

	B3LYP/6-311++G (3df,3pd)	B3LYP/6-311++G (d,p)	MP2/6-311++G (d,p)	B3LYP/ aug-cc-pvtz
I	0.00	0.00	0.00	0.00
TS I-II	15.55	15.15	14.75	15.46
II	4.15	3.62	3.11	4.12
III	13.35	13.96	12.83	13.34
TS III-V	28.92	29.37	28.34	28.79
V	17.78	18.13	17.00	17.70
TS V-IX	29.08	29.16	27.14	28.97
IX	24.29	24.56	22.47	24.13
TS IX-VIII	34.89	35.24	33.24	34.73
VIII	20.86	21.45	19.92	20.76
TS	26.51	26.89	25.34	26.39
VIII-III				
III	13.35	13.96	12.83	13.34
VIII	20.86	21.45	19.92	20.76
TS VIII-X	37.74	38.71	39.42	37.63
X	35.11	35.97	38.23	34.99
TS X-I	43.02	43.55	45.97	42.85
I	0.00	0.00	0.00	0.00
III	13.35	13.96	12.83	13.34
TS III-I	27.46	28.09	27.98	27.43
I	0.00	0.00	0.00	0.00

tautomers of these species were performed. Scheme 2 shows possible interchanges between those conformers and tautomers while Table 1 presents the relative energies for them. The energies are related to species I which is characterized by the lowest one. Table 1 contains also the energies of transition states.

Figures 1 and 2 present the results of B3LYP/aug-cc-pVTZ IRC calculations; for both figures, the intrinsic reaction coordinate is related to the energy of species. Additionally, the changes of bond lengths during the interchange processes are presented within the figures. In order to have a consistent picture (Figures 1 and 2), the conformation VIII is presented as the starting one. Thus, both figures present the possible intramolecular double PT for which there is the change of III into I moiety. Figure 1 presents the following steps of this process: III \rightarrow TS III-I \rightarrow IV \rightarrow IV' \rightarrow I. The B3LYP/aug-cc-pVTZ barrier height amounts to 14.1 kcal/mol (27.4 kcal/mol minus 13.3 kcal/mol; see Table 1). It is interesting that this is not a concerted process as, for example, for the intermolecular double PT for formic acid dimer. For conformation III there is the PT for the O-H...N hydrogen bonding leading to the O...H-N hydrogen bond within an unstable IV zwitterionic form. Next there is the other PT process which (through IV') leads to the conformation I.

Figure 2 presents a much more complicated path of change structure III into I. First, the interchange of III into VIII is needed through the process of rotation (III \rightarrow VIII, this is shown on the left side of Figure 1). Next, the following transformations occur: VIII \rightarrow TS VIII-X \rightarrow X \rightarrow TS X-I \rightarrow IV \rightarrow IV' \rightarrow I. It is worth mentioning that the last steps of this process go through unstable moieties, IV and IV'. This again is not a concerted process of the double proton transfer since at first the X and IV zwitterion forms are obtained as an effect of the O-H...N \rightleftharpoons O...H-N proton transfer. Next, there is the O-H...O \rightleftharpoons O...H-O reaction leading to the

(29) Reed, A. E.; Curtiss, L. A.; Weinhold, F. *Chem. Rev.* **1988**, *88*, 899.

(30) Bader, R. F. W.; MacDougall, P. J.; Lau, C. D. H. *J. Am. Chem. Soc.* **1984**, *106*, 1594.

(31) Smedarchina, Z.; Siebrand, W.; Fernández-Ramos, A. Multiple Proton Transfer: From Stepwise to Concerted. In *Hydrogen-Transfer Reactions*; Hynes, J. T., Klinman, J. P., Limbach, H.-H., Schowen, R. L., Eds.; Wiley-VCH Verlag GmbH & Co. KGaA: Weinheim 2009.

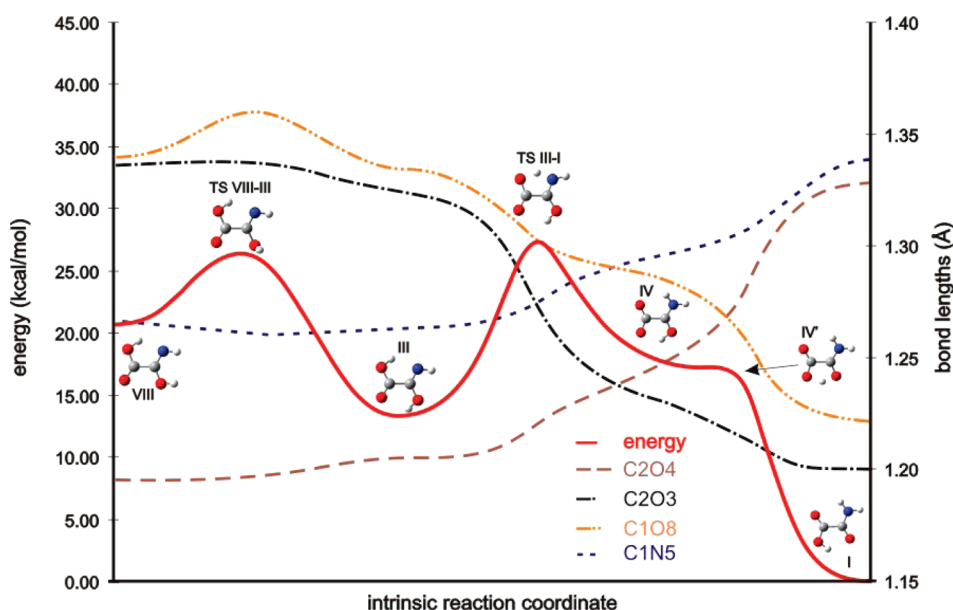


FIGURE 1. Different conformations and tautomers and their energies related to the intrinsic reaction coordinate path (IRC). The changes of bond lengths are also shown. The change of VIII into I by the double proton transfer reaction is presented (VIII–III–I).

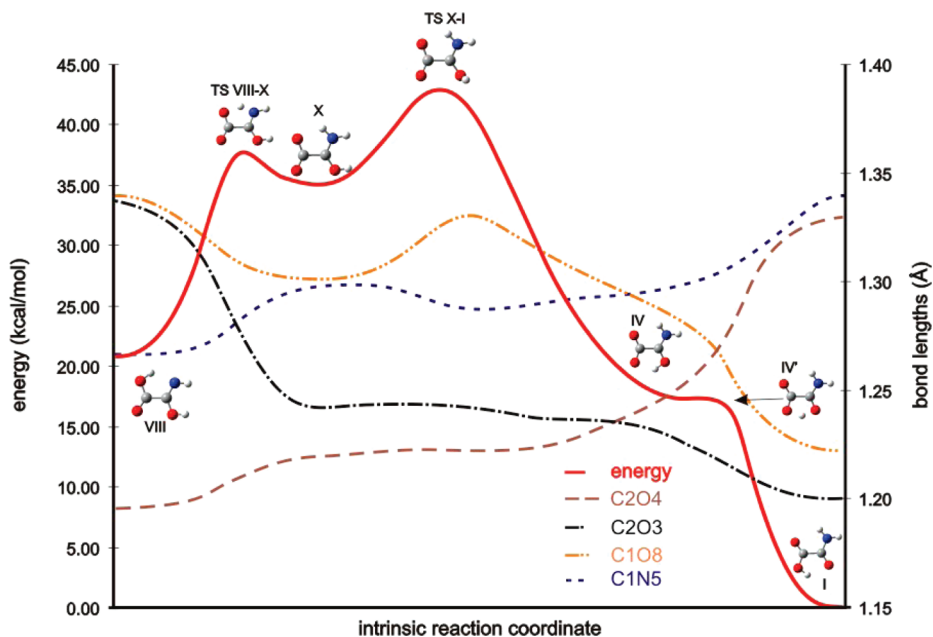


FIGURE 2. Different conformations and tautomers and their energies related to the intrinsic reaction coordinate path (IRC). The changes of bond lengths are also shown. The change of VIII into I by the double proton transfer reaction is presented (VIII–X–I).

final conformation I. Scheme 2, where all rotations and proton transfer reactions are designated, nicely corresponds to these figures. One can see from the scheme the only possible paths for the III–I transformation. The first path is as follows: III–PT–IV–PT–IV'–PT–I, and it corresponds to Figure 1. The second path is III–rotation–VIII–PT–X–rotation–IV–PT–IV'–PT–I, and this corresponds to Figure 2. Figures 1 and 2 also present the changes of bonds during these processes. One can see that during the first step of the $\text{O–H}\cdots\text{N} \rightleftharpoons \text{O}\cdots\text{H–N}$ proton transfer there is the C2–O3 bond shortening and the concerted elongation of the C1–N5 bond (for designations see Scheme 1). Similarly, during the next process ($\text{O}\cdots\text{H–O} \rightleftharpoons \text{O–H}\cdots\text{O}$) there is

the lengthening of the C2–O4 bond and shortening of the C1–O8 one.

Table 2 presents the geometrical parameters of hydrogen bonding interactions. There are no greater differences for various levels of approximations applied in this study. It is often assumed that the proton donor–acceptor and the proton–acceptor distances are rough descriptors of the hydrogen bonding strength.³² Hence, $\text{O–H}\cdots\text{O}$ hydrogen bonds are stronger than $\text{N–H}\cdots\text{O}$ interactions since $\text{N}\cdots\text{O}$ distances are greater than $\text{O}\cdots\text{O}$ ones and $\text{H}\cdots\text{O}$

(32) Jeffrey, G. A.; Saenger, W. *Hydrogen Bonding in Biological Structures*; Springer-Verlag: Berlin, 1990.

TABLE 2. Geometrical Parameters (in Å and deg) of the Species Considered Here, for Each Conformation the Results Obtained at Four Levels of Approximation Are Presented, in the Following Order (Four Lines for Each Conformation): B3LYP/6-311++G(3df,3pd), B3LYP/6-311++G(d,p), MP2/6-311++G(d,p), B3LYP/aug-cc-pVTZ

conformation	X–H···Y	X–H	H···Y	X···Y	X–H···Y
I, N–H···O	1.007	2.369	2.753	101.6	
	1.009	2.376	2.757	101.3	
	1.009	2.361	2.753	101.9	
	1.007	2.371	2.755	101.6	
I, O–H···O	0.977	2.019	2.639	119.4	
	0.978	2.027	2.646	119.2	
	0.976	2.009	2.648	121.1	
	0.978	2.017	2.640	119.5	
II, N–H···O	1.006	2.305	2.703	102.2	
	1.008	2.313	2.707	101.9	
	1.009	2.308	2.714	102.6	
	1.006	2.307	2.705	102.2	
III, O–H···N	0.978	2.068	2.671	118.0	
	0.979	2.065	2.671	118.2	
	0.977	2.041	2.669	120.2	
	0.978	2.067	2.671	118.1	
III, O–H···O	0.974	2.111	2.684	115.9	
	0.975	2.125	2.693	115.6	
	0.973	2.105	2.694	117.3	
	0.974	2.113	2.686	115.9	
IV ^a , N–H···O	1.018	2.212	2.689	106.8	
IV ^a , O–H···O	0.995	1.867	2.565	124.5	
V, O–H···O	0.972	2.062	2.643	116.5	
	0.973	2.072	2.650	116.2	
	0.971	2.059	2.655	117.9	
	0.972	2.062	2.644	116.6	
VI, N–H···O	1.015	2.304	2.764	106.2	
	1.017	2.299	2.765	106.4	
	1.019	2.284	2.771	107.8	
	1.019	2.306	2.765	106.1	
VII, N–H···O	1.015	2.346	2.810	106.6	
	1.018	2.338	2.810	107.0	
	1.020	2.303	2.809	109.2	
	1.015	2.347	2.811	106.7	
VII, O–H···O	0.969	2.097	2.670	116.2	
	0.970	2.111	2.681	116.0	
	0.968	2.097	2.686	117.5	
	0.970	2.098	2.672	116.2	
VIII, O–H···N	0.976	2.013	2.629	119.1	
	0.977	2.012	2.631	119.2	
	0.975	1.998	2.634	120.9	
	0.976	2.013	2.631	119.1	
X, N–H···O	1.027	1.969	2.552	113.0	
	1.029	1.985	2.565	112.8	
	1.031	1.934	2.543	114.7	
	1.027	1.967	2.553	113.2	

^aB3LYP/6-311++G(d,p) level of approximation.

distances for O–H···O bridges are shorter than these distances for N–H···O systems. Additionally, O–H···O angles are closer to linearity than N–H···O ones. In conformation I, both types of hydrogen bonds exist; the H···O distance of the O–H···O bridge is about 2.02 Å, the O···O distance is about 2.64 Å, and the O–H···O angle is equal to ~119°. The corresponding parameters for the N–H···O hydrogen bond are equal to ~2.37 Å (H···O), ~2.75 Å (N···O distance), and 101–102° (N–H···O angle). Only the N–H···O hydrogen bonding occurs for conformation II which seems to be stronger than the corresponding N–H···O interaction for I. The proton–acceptor distance for the conformation II is shorter than for I, the N···O distance is also shorter for II than for I and the N–H···O angle for II is greater. This may mean that for conformation I the existence of the extra O–H···O interaction causes the

weakening of the N–H···O hydrogen bonding. The same tendency occurs for conformations III and VIII. There are two interactions for III, O–H···N and O–H···O while for the conformation VIII only the O–H···N interaction exists. One can see that O–H···N for VIII is stronger than the corresponding hydrogen bonding for III (Table 2). Additionally, if one compares the O–H···N hydrogen bonding with the other N–H···O and O–H···O interactions the O–H···N belongs to the strongest interactions. It has the shortest proton–acceptor contacts as well as the greatest X–H···Y angles (X designates the proton donor while Y the proton acceptor). It is worth mentioning that if the following proton transfer reaction occurs (N–H···O ⇌ N···H–O), the hydrogen bonding of products of this process: O–H···N is stronger than the N–H···O interaction. This is in line with the Leffler–Hammond rule³³ that the system of higher energy and being closer to the transition state of the process generates stronger hydrogen bonding. Such a situation is also detected for conformations analyzed here (Scheme 2). The proton transfer O–H···N ⇌ O···H–N changes the conformation III into IV. However, the latter conformation is not a stationary point of IRC; only for B3LYP/6-311++G(d,p) level of approximation the conformation IV is the local minimum. Still, for all levels of approximation the geometrical results (Table 2) show that the O–H···N hydrogen bonding for III is stronger than N–H···O of IV. Similarly, the conformation VIII with the O–H···N hydrogen bonding is changed into X after the proton transfer process. The N–H···O hydrogen bonding is formed for X. Figure 2 shows that this conformation is closer to the transition state of the PT than the conformation VIII. Consequently, the N–H···O hydrogen bonding of X is stronger than the O–H···N interaction of VIII; this is also in line with the Leffler–Hammond rule. The latter finding is rather surprising since usually O–H···N hydrogen bonds are stronger than N–H···O ones. However, one can see that the N–H···O interaction occurs in X zwitterionic form and hence N–H···O may be classified as the charge assisted hydrogen bonding.

Interrelations between QTAIM, NBO, and Geometrical Parameters. One can see (Scheme 2, Table 2) that the conformations considered here usually possess X–H···Y intramolecular interactions. The conformation IX is the only exception where such contacts do not exist. The question arises if those X–H···Y systems may be classified as hydrogen bonds. Various methods and theories provide characteristics and criteria for the existence of the hydrogen bonding. From the geometrical point of view, the proton–acceptor distance should be smaller than the corresponding sum of van der Waals radii;³² it is ~2.6 and ~2.75 Å for H···O and H···N distances, respectively. Additionally, the X–H···Y angle tends to linearity; at least it should be greater than 90°. Table 2 shows that all H···Y distances fulfill the mentioned above condition, although X–H···Y angles are far from linearity, but all are greater than 90°. Various QTAIM criteria of the existence of the hydrogen bonding were proposed by Koch and Popelier.³⁴ Not all the

(33) (a) Leffler, J. E. *Science* **1953**, *117*, 340. (b) Hammond, G. S. *J. Am. Chem. Soc.* **1955**, *77*, 334.

(34) (a) Koch, U.; Popelier, P. L. A. *J. Phys. Chem. A* **1995**, *99*, 9747. (b) Popelier, P. *Atoms in Molecules. An Introduction*; Prentice Hall: Pearson Education Ltd., 2000.

TABLE 3. Characteristics of X–H···Y Interactions, Geometrical, NBO, and QTAIM Criteria Are Applied, H···Y Distances (in Å), $\Delta E(n_Y \rightarrow \sigma_{XH}^*)$ (in kcal/mol), ρ_{BCP} (in au)^a

species	type of interaction →	OH···O	NH···O	OH···N
I	existence of interaction	yes	yes	no
	existence of BCP	yes	no	
	ΔE	3.79		
	H···O	2.017	2.371	
	ρ_{BCP}	0.027		
II	existence of interaction	no	yes	no
	existence of CP		no	
	ΔE		0.55	
	H···O		2.307	
	ρ_{BCP}			
III	existence of interaction	yes	no	yes
	existence of CP	no		yes
	ΔE	2.38		3.74
	H···O(N)	2.113		2.067
	ρ_{BCP}			0.025
V	existence of interaction	yes	no	no
	existence of CP	no		
	ΔE	2.72		
	H···O	2.062		
	ρ_{BCP}			
VI	existence of interaction	no	yes	no
	existence of CP		no	
	ΔE			
	H···O		2.306	
	ρ_{BCP}			
VII	existence of interaction	yes	yes	no
	existence of CP	no	no	
	ΔE	2.12		
	H···O	2.098	2.347	
	ρ_{BCP}			
VIII	existence of interaction	no	no	yes
	existence of CP			yes
	ΔE			4.60
	H···N			2.013
	ρ_{BCP}			0.028
IX	existence of interaction	no	no	no
	existence of CP			
	ΔE			
	H···O			
	ρ_{BCP}			
X	existence of interaction	no	yes	no
	existence of CP		yes	
	ΔE		7.41	
	H···O		1.967	
	ρ_{BCP}		0.031	

^aQTAIM parameters are given in Supporting Information.

required terms are applied here. However, it is important that for the X–H···Y hydrogen bonding interaction at least the H···Y bond path should exist with the corresponding bond critical point (BCP). Table 3 summarizes selected geometrical, QTAIM, and NBO results (B3LYP/aug-cc-pVTZ level). One can see that the distance H···Y criterion may sometimes not correspond to QTAIM requirements of the hydrogen bonding existence. There are bond paths and bond critical points only in few cases of the mentioned above X–H···Y contacts. Thus generally for the species analyzed here the QTAIM criteria are not in line with the geometrical ones.

Table 3 also presents the $n_Y \rightarrow \sigma_{XH}^*$ interaction energies (ΔE – eq 1) which are often attributed to the existence of the hydrogen bonding interaction. For X–H···Y systems, only in three cases of N–H···O systems, i.e., for I, VI, and VII conformations, the ΔE energy is not detected. The greatest

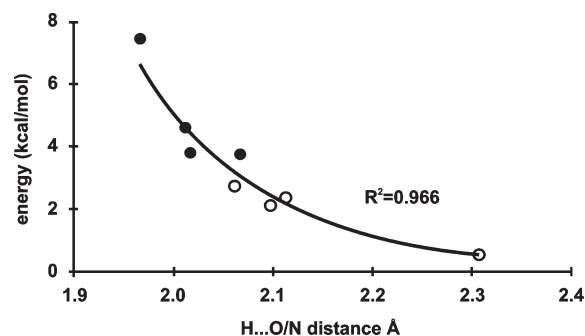


FIGURE 3. Relationship between the proton–acceptor distance (in Å, H···O or H···N) and the NBO energy (in kcal/mol) expressed by eq 1, the X–H···Y systems for which H···Y bond paths with corresponding BCPs were detected are designated as full circles.

H···Y distances for these moieties exist and are about 2.3 Å. In other words, the geometrical H···Y distance parameter is the most sensitive one to detect the hydrogen bonding existence while QTAIM is of the lowest sensitivity. Figure 3 presents the exponential relationship ($R^2 = 0.966$) between H···Y distance and ΔE energy expressed by eq 1. One can see that for the shorter H···Y distances there are critical points. In such cases ΔE energies are greater than 3.7 kcal/mol.

Table 3 also indicates another interesting relationship. The strongest intramolecular interactions occur if BCPs are detected. These interactions are classified as hydrogen bonds by geometrical, NBO, and QTAIM parameters. All these strong hydrogen bonds may be treated as preliminary stages of PT reactions. The first one is O–H···O interaction of the conformation I, after the “single” PT process (through IV') the conformation IV is obtained (Scheme 2). Only for B3LYP/6-311++G(d,p) level of approximation it is a stationary point. There is no B3LYP/aug-cc-pVTZ results for that system. The other strong hydrogen bonding fulfilling geometrical, QTAIM and NBO criteria (Table 3) is the O–H···N interaction of the conformation III; after the PT process one obtains the conformation IV with the N–H···O hydrogen bonding. The last two strong hydrogen bonds where BCPs were detected are interactions of conformations VIII and X interrelated through the O–H···N \leftrightarrow O···H–N PT process.

It is interesting that the X–H···Y interactions where BCPs are not detected do not take part in PT reactions. The latter results are in line with the statement that the hydrogen bonding interaction is the preliminary stage of the PT reaction.²⁰ However, recent studies do not show the direct interrelation between the PT process and the hydrogen bonding.²¹

Charge distribution on atoms participating in hydrogen bonding interactions is also interesting. Table 4 shows NBO atomic charges for the moieties analyzed here (B3LYP/aug-cc-pVTZ level of approximation). The designations of atoms correspond to those of Scheme 1. The H7 atom is involved in the O–H···N or N–H···O interaction, except for conformations V and IX where such contacts do not occur. The greatest positive charges on the H7 atom occur for conformations III and VIII where O–H···N hydrogen bonds exist which are stronger than N–H···O ones. The other hydrogen atom, H9, may participate in the O–H···O hydrogen bonding. The greatest positive charge on this atom occurs for conformations I, III, V, and VII—for those conformations where O–H···O interaction occurs (Scheme 2). There

TABLE 4. NBO Charges (in au) for the Species Analyzed Here

	C1	C2	O3	O4	N5	H6	H7	O8	H9
I	0.534	0.702	-0.562	-0.644	-0.759	0.402	0.416	-0.598	0.509
II	0.546	0.700	-0.586	-0.633	-0.773	0.399	0.414	-0.558	0.491
III	0.467	0.703	-0.645	-0.553	-0.711	0.363	0.514	-0.645	0.507
V	0.449	0.711	-0.633	-0.582	-0.621	0.345	0.494	-0.666	0.503
VI	0.467	0.699	-0.686	-0.513	-0.690	0.366	0.499	-0.628	0.486
VII	0.430	0.709	-0.658	-0.583	-0.604	0.354	0.499	-0.643	0.497
VIII	0.485	0.704	-0.661	-0.505	-0.738	0.348	0.508	-0.617	0.476
IX	0.470	0.706	-0.654	-0.527	-0.655	0.330	0.492	-0.635	0.474
X	0.594	0.705	-0.710	-0.624	-0.713	0.389	0.461	-0.577	0.477

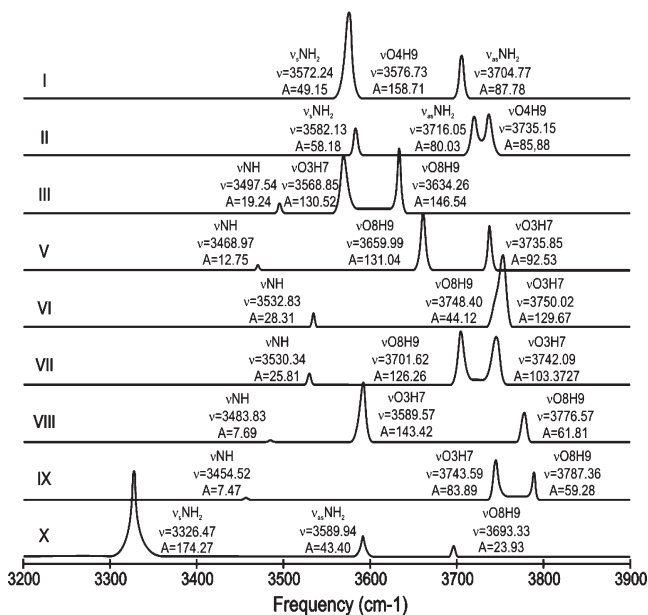


FIGURE 4. Stretching frequencies (in cm^{-1}) of N-H and O-H bonds and related modes' intensities for I-X species analyzed here (B3LYP/aug-cc-pVTZ level of approximation).

are not regular dependencies for proton donors' and proton acceptors' charges. For example, "the most negative" N5 atom occurs for the conformation I where N-H...O and O-H...O hydrogen bonds occur and which is of the lowest energy (Figures 1 and 2). The "most negative" O3 atom occurs for the conformation X. For that moiety the O3 atom is a proton acceptor within the strong charge assisted N-H...O hydrogen bonding. Additionally, the conformation X is a zwitterionic form thus the O4 atom also have relatively high negative charge. The most negative oxygen atom (O8) occurs for conformations: III, V, and VII. For these species O8 is involved in hydrogen bonding interactions as a proton donor.

Figure 4 presents the spectra of I-X structures considered here (B3LYP/aug-cc-pVTZ level of approximation), stretching frequencies and corresponding intensities of N-H and O-H bonds are given. There are maxima corresponding to free (not involved in X-H...Y interactions) O-H bonds on the right side of the figure. The O3-H7 bond not involved in intramolecular noncovalent interaction occurs for V, VI, VII and IX conformers. Similarly, the O4-H9 bond which is not involved in X-H...Y interaction is detected for the

conformation II, O8-H9 which does not participate in X-H...Y interaction occurs for VI, VIII, IX and X species. If one compares the stretching frequencies of the O-H bonds not involved in the intramolecular noncovalent interactions with those which participate in such interactions, the maximal red-shifts occur for O-H bonds of species I and III (involved in O-H...O interactions) and in the case of the conformation VIII where the O-H...N hydrogen bonding occurs.

The symmetrical and asymmetrical stretching frequencies of NH₂ group are also presented in Figure 4 (conformations I, II, and X). The maximal stretching frequencies shift to the red is observed for the N-H...O strong and charge assisted hydrogen bonding of the zwitterionic conformation X.

There is C=N-H arrangement of atoms for III, V, VI, VII, VIII, and IX species. In two cases, for conformations VI and VII, there are N-H...O intramolecular interactions. And in these two cases the stretching vibration frequencies are the greatest ones if compared with these values for the remaining species (III, V, VIII, and IX). This means that such N-H...O interactions may be classified as the intramolecular blue-shifting hydrogen bonds. One can observe the increase of intensities of these modes (VI and VII) compared to the intensities of other N-H modes (III, V, VIII, and IX species). It is worth mentioning that the blue-shifting hydrogen bonds were mostly detected for C-H...Y interactions.³⁵ However, sometimes other types of blue-shifting hydrogen bonds exist, these are N-H...Y, F-H...Y, P-H...Y, or Si-H...Y.³⁶ Thus, the intramolecular blue-shifting hydrogen bonds found here are not the common and often existing phenomenon.

Conclusions

It was found that the double intramolecular proton transfer reaction which transforms 2-hydroxy-2-iminoacetic acid into 2-amino-2-oxoacetic acid is not a concerted process but a stepwise one. Two paths for such a process were indicated (Figures 1 and 2). Different conformations and tautomers which were created during the aforementioned transformations usually indicate the existence of intramolecular interactions. Various criteria were applied here to determine if they could be classified as hydrogen bonds. The number of interactions which are classified as hydrogen bonds decreases in turn if the following criteria are applied: geometry, NBO methods, and QTAIM. Only for four species investigated here was the hydrogen bonding indicated by QTAIM since bond paths with corresponding BCPs were detected. It is interesting that the latter species may be also treated as the preliminary stages of the proton transfer reactions. For a few analyzed structures the intramolecular N-H...O interactions may be classified as the blue-shifting hydrogen bonds.

Supporting Information Available: QTAIM parameters (Table S1) and atom coordinates with absolute energies (Table S2). This material is available free of charge via the Internet at <http://pubs.acs.org>.

(35) Hobza, P.; Havlas, Z. *Chem. Rev.* **2000**, *100*, 4253.

(36) (a) Satonaka, H.; Abe, K.; Hirota, M. *Bull. Chem. Soc. Jpn.* **1987**, *60*, 953. (b) Hobza, P. *Int. J. Quantum Chem.* **2002**, *90*, 1071. (c) Li, X.; Liu, L.; Schlegel, H. B. *J. Am. Chem. Soc.* **2002**, *124*, 9636.